

MULTI-DISCIPLINARY ROBUST DESIGN OF VARIABLE SPEED WIND TURBINES

Edmondo Minisci*, Sergio

Campobasso

School of Engineering

University of Glasgow

James Watt S.B., G12 8QQ, Glasgow, UK

Email: {edmondo.minisci,sergio.campobasso}

@glasgow.ac.uk

Michele Dellantonio

Dipartimento di Ing. Elettrica

Universit  di Padova

via Gradenigo 6/A, 35131, Padova, Italy

Email: michele.dellantonio@studenti.unipd.it

Andrea Montecucco

School of Engineering

University of Glasgow

Rankine Building, G12 8LT, Glasgow, UK

Email: andrea.montecucco@glasgow.ac.uk

Massimiliano Vasile

Department of Mechanical & Aerospace

Engineering, University of Strathclyde

75 Montrose Street, G1 1XJ, Glasgow, UK

Email: massimiliano.vasile@strath.ac.uk

Abstract. This paper addresses the preliminary robust multi-disciplinary design of small wind turbines. The turbine to be designed is assumed to be connected to the grid by means of power electronic converters. The main input parameter is the yearly wind distribution at the selected site, and it is represented by means of a Weibull distribution. The objective function is the electrical energy delivered yearly to the grid. Aerodynamic and electrical characteristics are fully coupled and modelled by means of low- and medium-fidelity models. Uncertainty affecting the blade geometry is considered, and a multi-objective hybrid evolutionary algorithm code is used to maximise the mean value of the yearly energy production and minimise its variance.

Key words: Multi-Disciplinary Optimisation, Robust Design, Integrated System Design, Evolutionary Computation, Wind Energy, Aerodynamic and Electrical Optimisation.

1 Introduction

The development of new small wind turbine systems is usually carried out adopting an *uncoupled approach* to the design of the individual components. This procedure consists of initially neglecting several effects of the coupling between aerodynamic and/or electrical and/or mechanical components on the overall performance, and later performing an experimental or, more rarely, numerical verification of the complete design. This latter stage aims to achieve a suitable component integration. Following this approach, the blade geometry, the characteristics of the generator, and those of the inverter, which are the main sub-systems determining the power output, are obtained by separate design exercises^{1,2}. As a consequence, the subsequent component integration is time consuming and expensive, due primarily to the

financial and logistic requirements of suitable experimental campaigns, and also to last-minute design alterations aimed at improving component matching.

On the other hand, the use of a simulation-based *fully coupled* approach since early stages of the design would allow the wind energy industry to both reduce development costs and time-scales, and develop more efficient turbines. The benefits and the effectiveness of adopting the fully coupled design strategy since early stages of the product design have been known and exploited for a long time in other engineering fields such as aircraft³ and turbomachinery⁴ design. To the best of the author's knowledge, however, the development and the application of the fully coupled strategy for wind turbine conceptual and preliminary design have not been suitably explored yet.

The fully coupled design optimisation approach is computationally more demanding than the faster conventional uncoupled design strategy. However, the high performance of modern computers and the increasing availability of parallel computing resources allow numerical optimisation to handle complex multidisciplinary design problems in relatively short times. These circumstances presently enable one to model all the sub-systems using diverse fidelity levels and directly proceed with the integrated design of the whole system.

This paper presents an integrated approach to the preliminary multi-disciplinary robust design of small variable speed horizontal axis wind turbines. The attribute 'robust' stems from the fact that the effects of uncertainty such as that due to manufacturing and assembly tolerances on the objective functions and constraints is carefully taken into account in the design optimisation⁵. The turbines of the considered class have rated power of up to about 50 kW and feature a permanent magnet generator and an inverter. The multidisciplinary analysis system considered herein couples the aerodynamic and electrical characteristics of the turbine, and models them by means of low- and medium-fidelity models. The main input parameters are the yearly wind distribution at the selected site and the rotor swept area. The objective of the design optimisation is to maximise the yearly energy harvest. This quantity corresponds to the energy delivered to the grid, since it is assumed that the turbine system is directly connected to the grid. Given that the optimisation is carried out taking into account uncertainty of the design variables, the robust optimisation actually consists of maximising the mean of the yearly energy production and minimising its standard deviation. As shown in the remainder of this paper, this optimisation specifications result in the occurrence of a Pareto front.

The uncertainty affecting the design variables can be due to several stochastic factors, including manufacturing and assembly tolerances and wear. In the present study, the Univariate Reduced Quadrature (URQ) approach to uncertainty propagation in robust design optimisation is used⁶. The estimate of mean and variance of the objective function(s) and constraints based on the URQ approach is deterministic. The calculation of mean and variance of the stochastic output functional requires $2N + 1$ deterministic analyses, where N denotes the number of input variables on which the considered output functional depends. The article⁶ reports the robust shape design optimisation of a transonic airfoil. In this paper, the URQ approach is used to take into account the effect of normally distributed uncertainty of the design parameters defining the blade geometry. Such uncertainty propagates through the aerodynamic and electric model and results in the annual energy yield becoming a

stochastic variable, characterised by a mean and a standard deviation. In the robust optimisation process, the output of each robust analysis is used by a multi-objective evolutionary algorithm (EA), whose objectives are the maximisation of the mean value of yearly energy production and the minimisation of its variance.

The adopted EA hybridises the Multi-Objective Parzen based Estimation of Distribution (MOPED) algorithm^{7,8}, and the Inflationary Differential Evolution Algorithm (IDEA)⁹, where MOPED is used to explore the search space and converge to a preliminary approximation of the Pareto front, while IDEA is then adopted to further push some of the best solutions towards the true Pareto front.

The aerodynamic and electrical models are described in section 2, whereas the main features of the two adopted optimisers and their use in this work are reported in section 3. The set-up and the results of a wind turbine robust design optimisation are provided in section 4. Then, a conclusion section summarises the work and anticipate future developments.

2 System Models

The wind energy conversion system (WECS) considered in this paper can be divided into two main parts: an aerodynamic part and an electro-mechanical part. The former consists of the bladed rotor, while the latter is made up of a permanent magnet synchronous generator and power electronic converters.

2.1 Aerodynamic model

The aerodynamic module of the integrated analysis system is a blade-element momentum (BEM) theory code¹⁰, developed at the School of Engineering of Glasgow University. This low-fidelity analysis tool is based on the radial subdivision of the bladed rotor into sections or strips. The BEM model used in this work includes the wake rotation. For each strip, the flow data and the aerodynamic forces are determined by equating the thrust and the torque computed with the classical lift and drag theory on one hand, and the conservation of the one-dimensional linear and angular momentum on the other. Tip and hub vortex losses are also included by means of the Prandtl tip loss model. The aerofoil lift and drag coefficient data are stored in tables as functions of the Reynolds number and the relative angle of attack, and such data are computed in a pre-processing step using the MIT aerodynamic solver XFOIL.

The set of input variables of the BEM code is made up of: freestream wind velocity, angular speed of the rotor, number of blades and blade geometry. This latter is defined by root and tip radius, and radial distributions of chord and twist angle. The set of output variables includes: aerodynamic power, axial thrust on the rotor, bending moment at the blade root and radial distributions of all flow data (e.g. axial and circumferential induction factors) and aerodynamic forces. As pointed out in the remainder of the paper, a single and constant aerofoil geometry is used throughout the design optimisation, and for this reason the lift and drag coefficient tables can be computed in a preprocessing step.

2.2 Electrical Model

The electro-mechanical model have specifically been implemented to be coupled to the aerodynamic module, so as to obtain a realistic prediction of the energy that

can be fed into the grid. For small wind turbines, permanent-magnet synchronous generators (PMSGs) offer significant benefits over induction generators: higher performance, gearbox-less operation, lower weight and smaller size¹¹. Therefore the main component of the electrical model is a PMSG to convert mechanical energy into electrical energy. The choice of the power electronics for interfacing such a generator to the grid is based both on the control requirements of an actual system and on the speed and easiness of the simulation.

A diode bridge rectifier is chosen for the greater simplicity of its control with respect to that of a controlled AC/DC converter. A grid-side inverter controls the reactive and active power supplied to the grid¹². The incorporation of a DC/DC converter in between the rectifier and the inverter enables one to achieve the following benefits^{14,13,15}:

1. Tight control of the generator-side voltage to achieve rotor speed control
2. Increase of voltage operating range while maintaining appropriate inverter-side DC voltage
3. Ease and flexibility of the inverter control
4. Reduced losses with Selective Harmonic Elimination (SHE)

A boost chopper is chosen as DC/DC convert and the described configuration is showed in Figure 1. It is assumed that there is infinite short-circuit power at the connection node, i.e. the voltage at this node is considered constant, and the iron core saturation and losses of the PMSG are neglected, as they are usually much smaller than the other losses. The model is implemented in Simulink using the SimPowerSystems toolbox (Figure 2 shows the Simulink model).

The inverter control can be designed to keep the DC-link voltage V_{DC2} constant

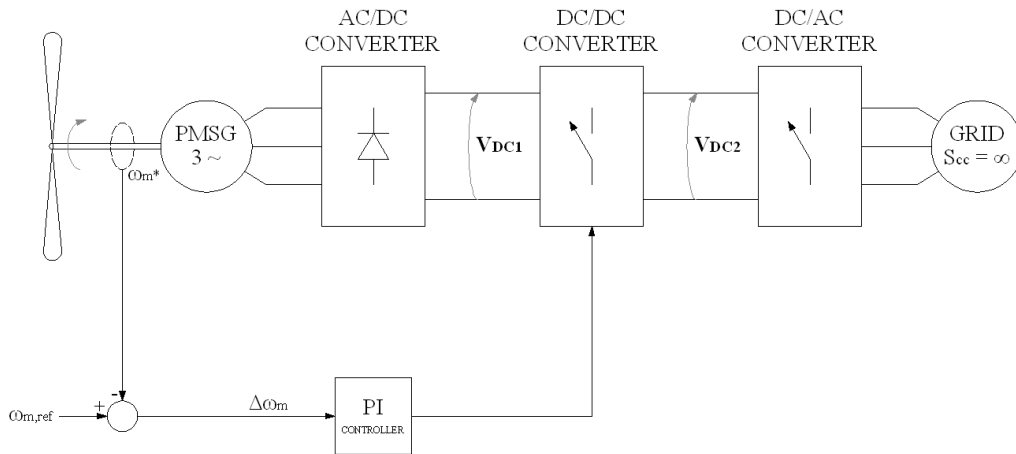


Figure 1: Diagram of the whole electro-mechanical system

varying the reactive power to maximise the real power supplied to the grid¹⁶. Therefore the output voltage of the boost converter is constant so that regulating its duty cycle (d) it is possible to control the rectifier output V_{DC1} using the relationship

$$d = \frac{V_{DC2} - V_{DC1}}{V_{DC2}} \quad (1)$$

Thus the voltage at the PMSG's terminals, which influences the rotor speed, can be controlled by a Maximum Power Point Tracking (MPPT) algorithm, which decides what operating mechanical speed to use in order to maximise the overall power produced by the system. The MPPT control is performed by the actual operating WECS, and not during simulation. For this reason and in order to make the simulation faster, the electrical system downstream of the diode rectifier has been modelled as an ideal DC voltage source, whose voltage is controlled depending on the desired mechanical speed requested by the optimiser.

The input variables of the electrical model are the mechanical speed $\omega_{m,ref}$ (rad/s) and the torque T_m (Nm), which come from the BEM code. A PI controller is used to impose the mechanical speed while the torque is directly set in the PMSG block. The PI controller regulates V_{DC1} in order to set the desired speed. The considered parameters for the PMSG are the number of poles p , the flux induced in the stator windings by the magnets ϕ (Wb), the nominal voltage V_n (V) and the maximum electrical frequency $f_{e,max}$. The parasitic effects of the components are constant and estimated from commercially-available components.

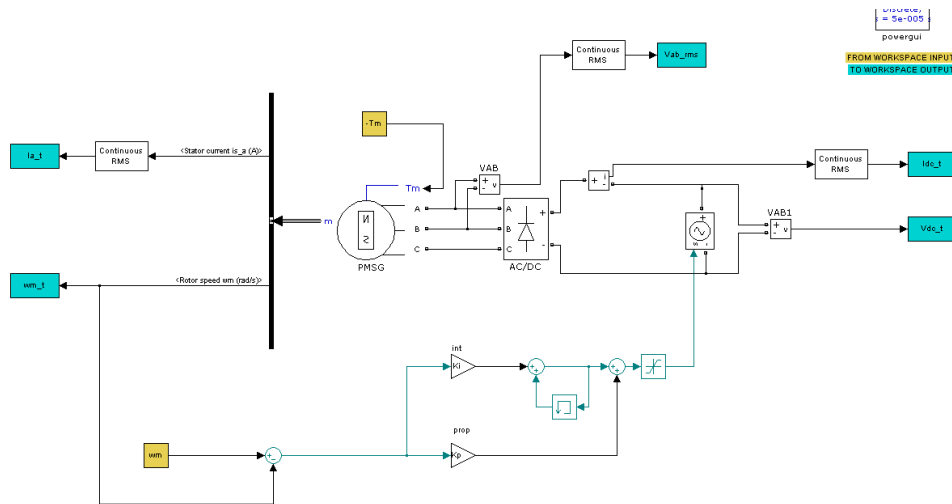


Figure 2: Simulink model

Before reaching steady-state, the simulation encounter a transient, whose time is function of the electrical (resistances, capacitances and inductances) and mechanical (torque and inertia) parameters (Figure 3). The output variables of the Simulink model are the mechanical speed $\omega_m^*(t)$, the DC bus voltage $V_{dc1}(t)$, the PMSG phase current $I_{a,RMS}$, the PMSG phase-to-phase voltage $V_{ab,RMS}$, and the DC bus current I_{DC} . After the simulation, losses are classified and computed as follows:

- mechanical losses due to viscous friction:

$$P_{l,m} = b\omega_m^{*2}$$

where $b(Nms)$ is the viscous friction coefficient;

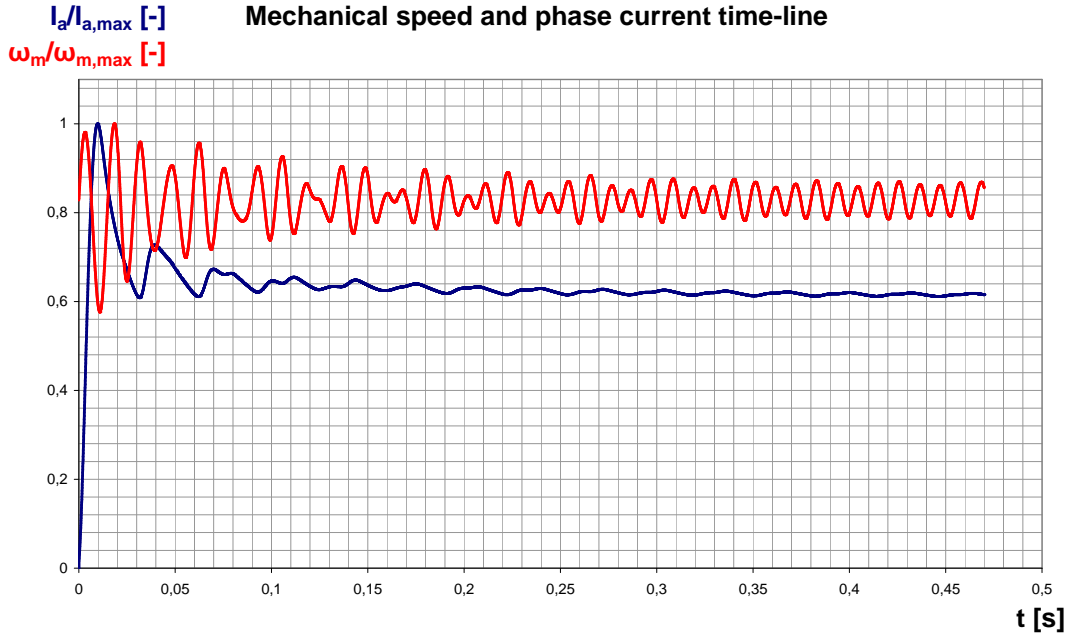


Figure 3: Mechanical speed and phase current time-line (model input: $\omega_m = 7 \frac{rad}{s}$, $T_m = 3300 Nm$)

- losses of the PMSG and rectifier:

$$P_{l,AC} = [3(R_s + R_{line}) + 2R_{br}]I_{a,RMS}^2$$

where R_s and R_{line} are the PMSG winding resistances and R_{br} is the resistance modeling the conduction losses on the diode bridge rectifier;

- losses on the DC/DC converter:

$$P_{l,L} = R_{DC} I_{DC}^2$$

$$P_{l,s} = R_{sw} (I_{DC} \sqrt{D})^2$$

$$P_{l,d} = R_d (I_{DC} \sqrt{1-D})^2$$

where R_{DC} is the inductor resistance, R_{sw} is the switch on-resistance and R_d is the diode conduction resistance; //

- losses on the inverter:

$$P_{l,inv} = (1 - \eta_{inv})(V_{DC1} I_{DC} - P_{l,L} - P_{l,s} - P_{l,d})$$

where η_{inv} is the inverter efficiency, which is assumed to be constant in the project operative range.

Once the losses have been determined, the electric model computes several intermediate efficiencies and the total one as:

- PMSG and rectifier efficiency:

$$\eta_{AC} = \frac{V_{DC1} I_{DC}}{P_m}$$

- DC/DC converter efficiency:

$$\eta_{DC} = \frac{1}{1 + \frac{V_d}{V_{DC}^2} + \frac{[R_{DC} + DR_{sw} + (1 - DR_d)] I_{DC}}{V_{DC}^2}}$$

where V_d is the forward voltage of the diode;

- total efficiency:

$$\eta_{tot} = 1 - \frac{\sum P_p}{P_m}$$

The outputs of the model are the total efficiency of the electrical system η_{tot} and the power supplied to the grid P_{grid} .

2.2.1 Model validity boundaries

In order to have feasible solutions, the PMSG nominal voltage V_n and the maximum electrical frequency $f_{e,max}$ must be bounded by the actual limits of a physical system. From V_n and $f_{e,max}$ depend other design parameters, such as the number of pole pairs p and the flux ϕ . The nominal voltage is the maximum voltage that the synchronous machine can generate. This parameter affects the winding insulation required and the output current; with a higher voltage, the current and thus the losses are lower, but a high voltage requires a great number of poles and a high flux. In a real PMSG the maximum frequency is imposed by the iron losses, and by the skin effect in the winding conductors. The former is the sum of hysteresis and eddy currents losses, $P_{l,iron} = k_{hy} f \hat{B}^2 + k_{ec} f^2 \hat{B}^2$, while the latter is characterised by the depth of penetration $\delta = \sqrt{\frac{\rho}{\pi f_e \mu_0}}$. If the frequency is high, then δ is small and the current flows in the conductor surface, increasing the Joule losses. Therefore a limit on the frequency value is necessary to avoid that a possible optimum configuration demands a high value of f_e . A minimum frequency $f_{e,min}$ is required too, because the generator cannot work with small frequencies. For these reasons V_n is the maximum voltage at the PMSG's terminals and $f_{e,min} \leq f_e \leq f_{e,max}$.

Therefore the following boundaries must be considered:

- mechanical speed range: $\omega_{m,min} \leq \omega \leq \omega_{m,max}$;
- mechanical power range: $P_{m,min} \leq P_m \leq P_{m,max}$;
- mechanical torque: $T_{m,min} \leq T_m \leq T_{m,max}$

where

$$T_{m,min} = \frac{P_{m,min}}{\omega_{m,max}} \quad T_{m,max} = \frac{P_{m,max}}{\omega_{m,min}} \quad (2)$$

These relationships allow to estimate the range of the parameters $p \in [p_{min}, p_{max}]$ and $\phi \in [\phi_{min}, \phi_{max}]$ as

$$p_{min} = \frac{2\pi f_{e,min}}{\omega_{m,max}} \quad p_{max} = \frac{2\pi f_{e,max}}{\omega_{m,min}} \quad (3)$$

$$\phi_{min} = \frac{V_n}{\sqrt{3} \omega_{m,max} p_{max}} \quad \phi_{max} = \frac{V_n}{\sqrt{3} \omega_{m,min} p_{min}} \quad (4)$$

where the RMS value of the fundamental EMF induced in the stator windings is $E = \frac{V_n}{\sqrt{3}} = p\phi\omega_m$.

The parameters V_n and $[f_{e,min}, f_{e,max}]$ are imposed as boundaries, while p and ϕ are considered values to optimize. For each values of torque and mechanical speed, the program starts the simulation searching for the values of p and ϕ that maximise the electrical energy produced in one year.

First, the MATLAB script calculates the PMSG's voltage V and electrical frequency f_e and checks that they are not outside the imposed boundaries, using the relationships

$$f_{e,min} \leq \left(f_e = \frac{p\omega_m}{2\pi} \right) \leq f_{e,max} \quad (5)$$

$$V = \sqrt{3}p\phi\omega_m \leq V_n \quad (6)$$

If the boundaries are satisfied, the simulation starts, otherwise the program returns a value of injected power to the grid P_{grid} calculated as

$$P_{grid} = \frac{P_m}{10 \frac{|\Delta f|}{f_{e,max}} \frac{|\Delta V|}{V_n}} \quad (7)$$

where Δf and ΔV are the difference between the imposed limit (of frequency and/or voltage) and the calculated values using Eq. 5 and 6.

It is not possible to reach steady-state with high values of mechanical torque T_m and/or low values of mechanical speed ω_m , ϕ or p . In these cases the mechanical speed does not converge to the set value $\omega_{m,ref}$ because the PMSG cannot generate the requested voltage to "brake" the rotor at the requested low speed and high torque. Vice versa, when the required speed is too high for the set torque value it is possible to reach steady-state, but with a lower mechanical speed than the reference $\omega_{m,ref}$. The mean value of the effective mechanical speed ω_m^* is computed and compared to the reference speed ω_m . If the difference satisfies the equation $\Delta\varpi = |\omega_m^* - \omega_m| \leq \frac{\omega_m}{5}$ then the program computes the losses and the power P_{grid} , otherwise the program sets $P_{grid} = \frac{T_m\omega_m^*}{|\Delta\varpi|}$. These two conditions are important for the correct functioning of the optimizer when it falls into those particular cases.

3 Evolutionary Hybrid solver

As previously stated, the adopted solver is an hybrid code which uses MOPED and IDEA, both previously developed by some of the authors in the framework of aerospace design and optimisation field.

The MOPED (Multi-Objective Parzen based Estimation of Distribution) algorithm is a multi-objective optimisation algorithm for continuous problems that uses the Parzen method to build a probabilistic representation of Pareto solutions, with multivariate dependencies among variables^{7,8}. Some techniques of NSGA-II¹⁷ are used to classify promising solutions in the objective space, while new individuals are obtained by sampling from the Parzen model. NSGA-II was identified as a promising base for the algorithm mainly because of its intuitive simplicity coupled with excellent results on many problems.

The Parzen method⁷ pursues a non-parametric approach to kernel density estimation and it gives rise to an estimator that converges everywhere to the true

Probability Density Function (PDF) in the mean square sense. Should the true PDF be uniformly continuous, the Parzen estimator can also be made uniformly consistent. In short, the method allocates N_{ind} identical kernels (where N_{ind} is the number of individuals of the population of candidate solutions), each one centred on a different element of the sample.

By means of the Parzen method, a probabilistic model of the promising search space portion is thus built on the basis of the information given by N_{ind} individuals of the current population, and $\tau_E N_{ind}$ new individuals ($\tau_E \geq 1$) can then be sampled. The variance associated to each kernel depends on (i) the distribution of the individuals in the search space and (ii) the fitness value associated to the pertinent individual, so as to favour sampling in the neighbourhood of the most promising solutions. In order to improve the exploration of the search space it is sometimes useful to alternatively adopt two different kernels when passing from one generation to the following one.

The nature itself of the algorithm often prevents the precise reaching of the Pareto front. Especially when the front is broad and individuals of the population are spread over different and far areas in the domain space. From here the idea to couple MOPED with another advanced evolutionary algorithm, which has better convergence properties.

For design and optimisation in other engineering areas, some of the authors developed an improved version of differential evolution (DE). The new algorithm, IDEA, is based on a synergic hybridisation of a differential evolution variant and the logic behind monotonic basin hopping (MBH)¹⁸. The resulting algorithm demonstrated to outperform DE and MBH on some difficult space trajectory design problems, whose search space has a (multi) funnel like structure. In this work a modified version of IDEA will be used to push individuals lying on the approximated Pareto front resulting from MOPED process, further toward the true front.

The main algorithm of IDEA is detailed in literature⁹, while here we will just recall the practical aspects of the algorithm. Basically, a DE process is performed several times and each process is stopped only when the population contracts under a predefined threshold. Every time that the DE stops, a local search is performed in order to properly converge to the local optimum. Since for non-trivial functions it is extremely easy to converge to only local optima, the DE+local search is iterated several times, considering either local restart or a global one, on the basis of a predefined scheduling.

For this work, since the optimisation is constrained, the internal DE mechanism must be modified and the comparison of individuals during the DE process must take into account constraints as well. Constraint handling technique in this case is borrowed from what usually done in evolutionary computation and also in MOPED. Basically, when parents and offsprings are compared, offsprings are chosen if they have a better constraint compatibility, cp , and in case cp of offspring and parent is the same (when the constraints are satisfied both for the parent and the children), then the objective function is considered.

When MOPED reaches the maximum number of generations, clustered sub-populations from the current front are given to IDEA as initial solutions. Since IDEA is still single objective, individuals picked up from final MOPED population are pushed forward considering a weighted sum of the original objective functions.

The use of the hybrid code is here justified by the fact that the structure of the

current problem is totally unknown, and could be multi-funnel like and extremely noisy. Noise is expected to be introduced by both the aerodynamic and the electric solvers. The adopted code, by mixing the exploratory capabilities of MOPED and the convergence characteristics of IDEA, should guarantee a satisfying robustness.

4 Optimisation setting and results

The turbine blade shape is parametrised by means of 6 design parameters defining the radial chord distribution, and 6 design parameters defining the radial twist distribution. Additional parameters define the rotational speed for each considered wind speed, as well as poles and flux for the design of the generator. Since in this case we considered 7 wind speeds from $6m/s$ to $12m/s$, the total number of design parameters is 21. Bounds for design parameters are given in Table 1. Internal and external blade radius are not allowed to change and fixed to $1.3[m]$ and $6.3[m]$, respectively.

$x_{1,2,3}$	$\in [0.10, 0.90] [m]$
x_4	$\in [0.10, 0.60] [m]$
x_5	$\in [0.10, 0.50] [m]$
x_6	$\in [0.10, 0.40] [m]$
$x_{7,8}$	$\in [10, 50] [deg]$
x_9	$\in [5, 50] [deg]$
x_{10}	$\in [0, 20] [deg]$
$x_{11,12}$	$\in [0, 0.5] [deg]$
x_{13-19}	$\in [50, 150] [rpm]$
x_{20}	$\in [4, 38]$
x_{21}	$\in [0.61, 8.27] [Wb]$

Table 1: Bounds of design parameters

Parameters to be set for the MOPED algorithm are size of the population, N_{ind} , number of constraint classes, N_{cl} , the fitness parameter, α_f , the sampling proportion, τ_E , and, in this case, they were set as: $N_{ind} = 100$, $N_{genMAX} = 100$, $N_{cl} = 3$; $\alpha_f = 0.5$; $\tau_E = 1$.

Since the adopted algorithms are built to minimise objective functions, the problem is set in order to have two objectives to minimise:

$$\begin{aligned} F_1 &= 1e6 - E_{TE} \\ F_2 &= \sigma_{TE}^2 \end{aligned} \quad (8)$$

where E_{TE} and σ_{TE}^2 are the mean value of the annual energy production ([kWh]) and its variance, respectively.

While, considered constraints are:

$$\begin{aligned} C_1 &: F_1 \leq 9.6e5 \\ C_2 &: F_2 \leq 2e7 \\ C_3 &: E_{M_B} \leq 12 \end{aligned} \quad (9)$$

where M_B is the bending moment ([kNm]) at the blade root and E_{M_B} is its mean value.

In order to compute statistical values to be used as objective and constraint functions, parameters defining the blade geometry are supposed to be uncertain parameters with gaussian distributions, centred on nominal values of parameters and have a standard deviation $\sigma = 0.03$ (it must be noted that all the solvers work on a non-dimensional search space, where all variables vary $\in [0, 1]$). Since only the 12 parameters defining the shape of the turbine blade are considered affected by uncertainty, and the deterministic sampling method requires $2n + 1$ evaluations, then, for this test case, each solution evaluation actually requires 25 computations of the full annual energy production⁶.

Parameters of DE in IDEA are set as: weighting factor, $F = 0.9$, crossover probability, $CR = 0.9$, strategy “*DE/best/1/bin*”. IDEA stops when the population contracts to 25% of maximum expansion during the evolution.

Considered speeds and relative cumulative timing to compute the annual energy production are shown in Figure 4, and are derived considering a weibull distribution with scale parameter $\lambda = 7$ and shape parameter $k = 2$.

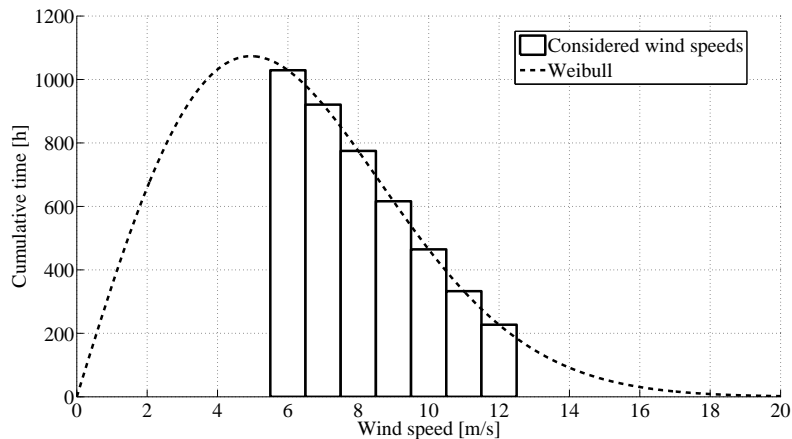


Figure 4: Wind speeds and cumulative timing considered to compute the annual energy production

4.1 Optimisation results

The whole code is implemented in MATLAB[®] and parallelised on a linux cluster, in order to speed-up the optimisation process.

After 10k function evaluations MOPED is able to approximate the Pareto front as shown in Figure 5. Pareto solutions were clustered in the search space and the sub-population containing the solution minimising F_1 was considered as the initial population of IDEA. After near 140 iterations of DE, which stops when the population contracts under the predefined threshold (see Sec. 3), and near 400 function evaluations of the local *fmincon* search, IDEA is able to find the solution marked with “**x**”. As can be seen, MOPED is able to explore the search space and converge to the region of optimal solutions, but the structure of the probabilistic model used to sample the search space, prevents it to further proceed. Likely, final optimal solutions are so spread that further sampling from the Parzen model was inefficient. Moreover, MOPED still appears too relying on solutions, which are no more good approximations of the front (left-upper corner). On the other hand, IDEA is able to refine the solution, improving the annual production of 3300kWh.

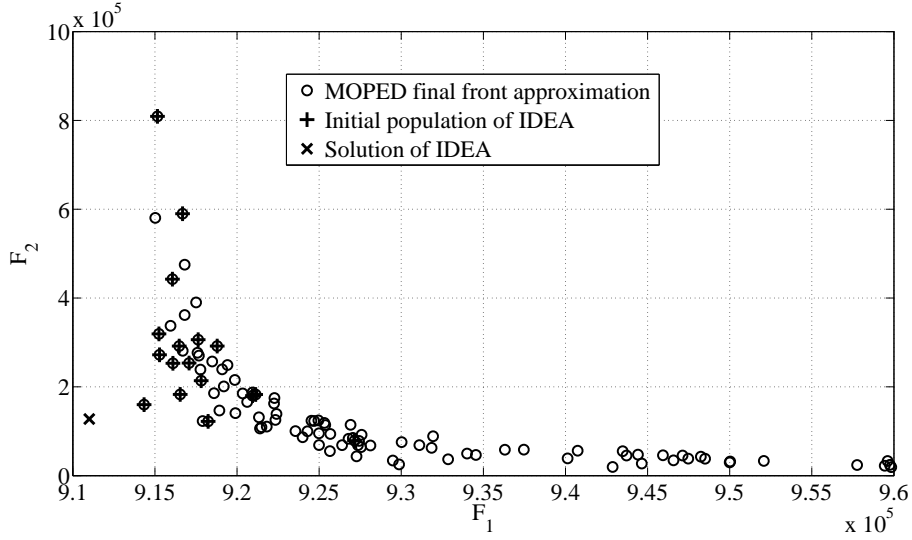


Figure 5: Solution of the optimisation process: Pareto front approximation found by MOPED, and final solution of the whole process after IDEA refinement.

At this point it is worth considering the cost of the refinement. If we take into account that the dimension of DE population was 17, the DE refinement required near 2400 evaluations, and that each function evaluation of *fmincon* includes the approximation of the local gradient, then the refinement of just one solution costed near 11k function evaluations, most of which required by *fmincon* to improve the solution of just 60 kWh. The deterministic sampling⁶ allows to efficiently compute the gradients of statistical values, but in this case we used *fmincon* to approximate them. Future tests will allow to compare performance when gradients are computed directly by the deterministic sampling and by *fmincon*.

The geometry of the optimal blade is shown in Fig. 6, while Figures 7 and 8 show the power curve of the turbine and the one referred to the entire chain up to the grid, respectively. Note that here the nominal results referred to the nominal blade are shown, which are not the statistical values considered by the searching codes.

It appears that the obtained solution should at rotational speeds maximising the power to the grid for each velocity, with some exceptions. In particular, operational point for $V_w = 10m/s$ is extremely close to the validity limit of the electric model, and that can disturb the computation of statistical values, preventing the nominal blade working at maximum power. Moreover, the machine cannot work at maximum power for $V_w = 12m/s$ due to the constraint on the maximum root bending moment, and a working point different from the maximum one must be adopted.

Final optimal point has the second objective function of just $127500 kWh^2$, meaning a standard deviation as small as $357kWh$. This result was obtained further refining a solution sampled from the MOPED final population, without considering the variance of the energy.

In Figure 9 the characteristic power curves for the optimal turbine are shown: the one considering just the turbine and the curve considering the turbine coupled to the electrical system. It can be seen that, for each curve, nominal values (dashed line) and mean values (continuous line) are almost coincident and standard deviations are very small, ranging from $0.035kW$ for lower powers to $0.27kW$ for higher powers.

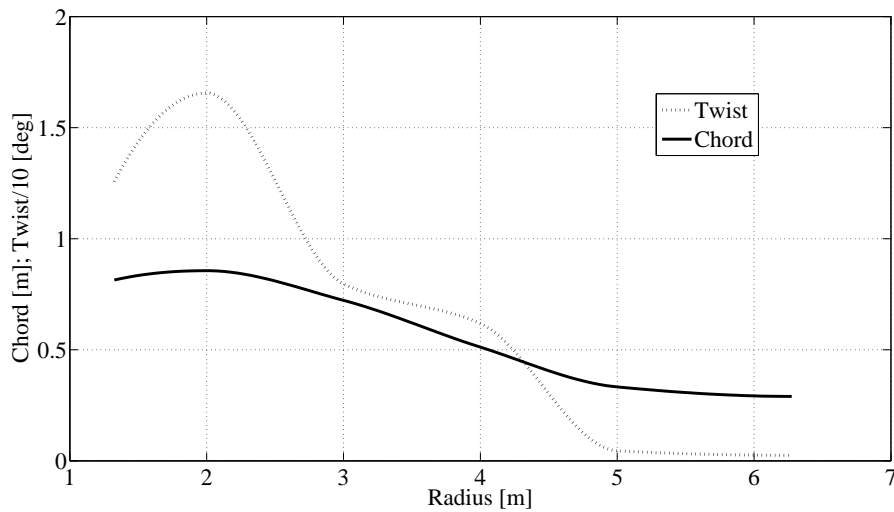


Figure 6: Nominal shape of the blade maximising the annual energy production as resulting from single objective refinement by IDEA

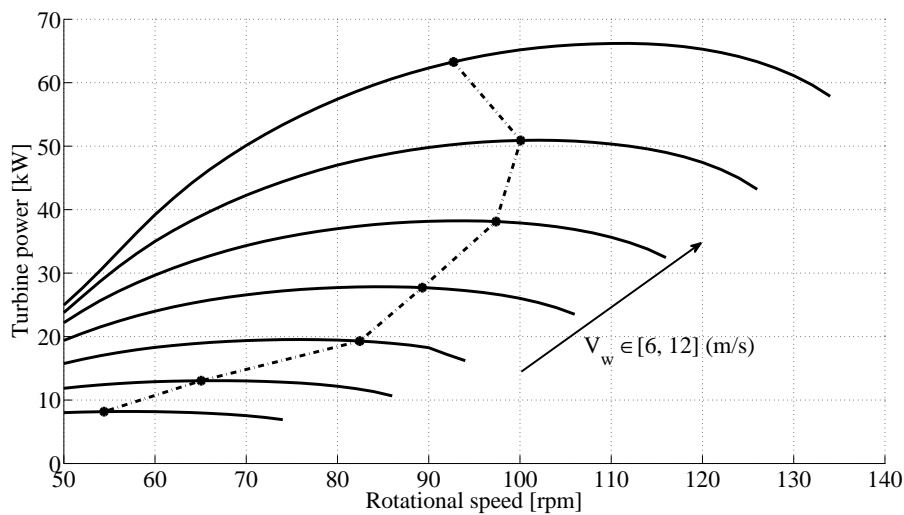


Figure 7: Turbine power curves of the nominal optimal blade

5 Conclusions

A hybrid evolutionary algorithm has been applied to the integrated robust design of a wind turbine system to maximise the annual energy production. Aerodynamic and electric components have been modelled and coupled to predict the energy that can be feeded to the grid.

The work demonstrates that such integrated approach is now possible, due to advances in evolutionary techniques and, overall, increased performance of modern computational systems, and it can be fruitfully used as main tool for preliminary design of wind systems. Nonetheless, the whole robust design approach remains computationally demanding and does not allow to run the code several times, as it should be done when dealing with stochastic solvers.

Immediate future work will be done to improve the electric modelling in order to obtain a higher fidelity model, and reduce the computational time. Long term

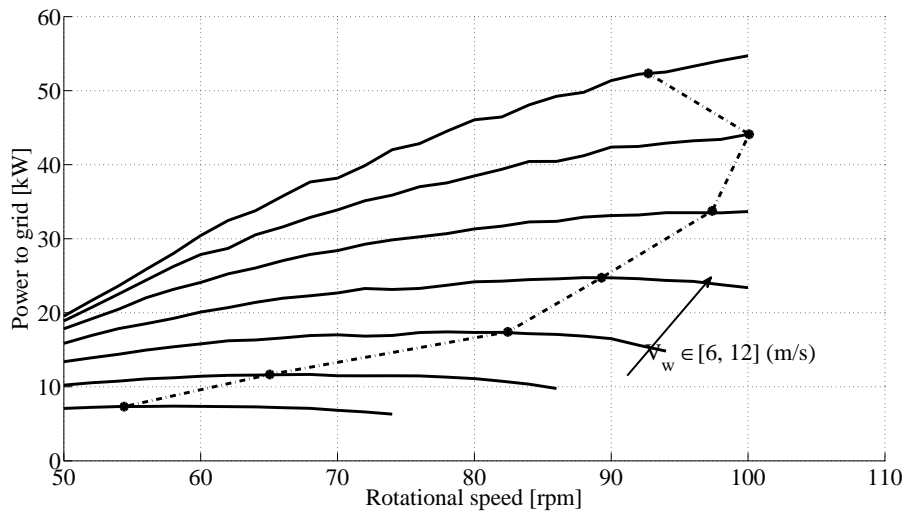


Figure 8: Power curves of the total system, considering the turbine and the electric chain up to the grid

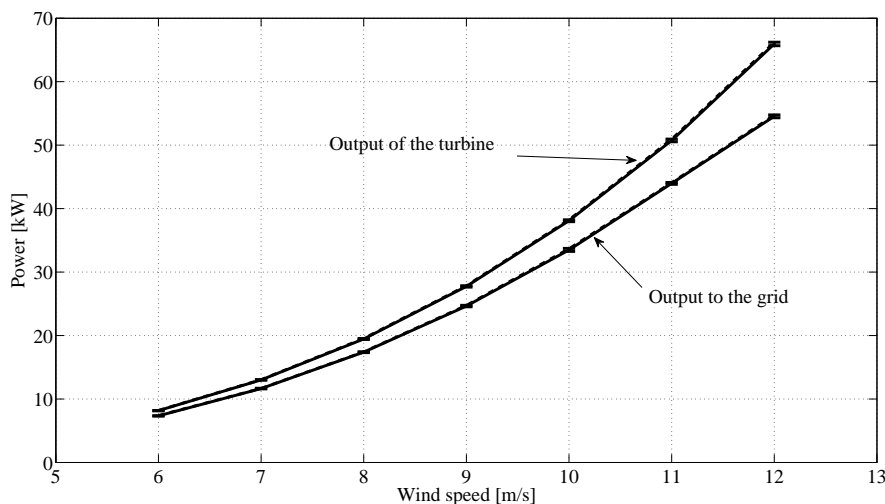


Figure 9: Power curve of the total system: maximum power as function of the wind speed

work will be focused on inserting into the process a multi-fidelity method as well as meta-modelling techniques. Moreover, in order to obtain realistic blade shapes with lower computational costs, the parametrisation of the blade should also consider manufacturing criteria and costs.

REFERENCES

- [1] A. Rolan, A. Luna, G. Vazquez, D. Aguilar and G. Azevedo, Modeling of a Variable Speed Wind Turbine with a Permanent Magnet Synchronous Generator, *IEEE International Symposium on Industrial Electronics (ISIE 2009)*, Seoul Olympic Parktel, Seoul, Korea July 5-8 (2009).
- [2] S. Bequé, J. Dils and M. Van Dessel, Optimisation of a direct drive low speed permanent magnet wind generator, *Proceedings of the Nordic MATLAB Conference 2003*, Copenhagen, Denmark, 215–219, October 21-22 (2003).

- [3] I. Kroo, S. Altus, R. Braun, P. Gage and I. Sobieski, Multidisciplinary Optimization Methods for Aircraft Preliminary Design, *Fifth AIAA/USAF/NASA/ISSMO Symposium on Multidisciplinary Analysis and Optimization Panama City*, AIAA 94-4325, Florida, September 7-9 (1994).
- [4] Y. Panchenko, H. Moustapha, S. Mah, K. Patel, M.J. Dowan and D. Hall, Preliminary Multi-Disciplinary Optimisation of Turbomachinery Design, *RTO AVT Symposium on 'Reduction of Military Vehicle Acquisition Time and Cost through Advanced Modelling and Virtual Simulation'*, RTO-MP-089, Paris, France, 22-25 April (2002).
- [5] G.J. Park, T.H. Lee, K.H. Lee and K.H. Hwang, Robust Design: An Overview, *AIAA Journal*, **44**(1), 181-191, (2004).
- [6] M. Padulo, M.S. Campobasso and M.D. Guenov, A Novel Uncertainty Propagation Method for Robust Aerodynamic Design, *AIAA Journal*, **49**(3), 530-543, (2011).
- [7] M. Costa and E. Minisci, MOPED: a multi-objective Parzen-based estimation of distribution algorithm, *In Proc. of EMO 2003*, Faro, Portugal, 282-294, (2003).
- [8] G. Avanzini, D. Biamonti, and E.A. Minisci, Minimum-fuel/minimum-time maneuvers of formation flying satellites, *Adv. Astronaut. Sci.*, **116**(III), 2403-2422, (2003).
- [9] M. Vasile, E. Minisci and M. Locatelli, An Inflationary Differential Evolution Algorithm for Space Trajectory Optimization, *Evolutionary Computation, IEEE Transactions on*, **15**(2), 267-281, (2011).
- [10] J. Manwell, J. McGowan, and A. Rogers, *Wind Energy Explained. Theory, Design and Application*, John Wiley and Sons Ltd., (2002).
- [11] M. Heydari, A. Yazdian Varjani, M. Mohamadian, and H. Zahedi, A Novel Variable-Speed Wind Energy System Using Permanent-Magnet Synchronous Generator and Nine-Switch AC/AC Converter. *2nd Power Electronics, Drive Systems and Technologies Conference, 2011*, 5-9, (2011).
- [12] S.H. Song, S.I. Kang, and N.K. Hahm, Implementation and control of grid connected AC-DC-AC power converter for variable speed wind energy conversion system. *Eighteenth Annual IEEE Applied Power Electronics Conference and Exposition, 2003. APEC '03.*, 00(C), 154-158, (2003).
- [13] J.A. Baroudi, V. Dinavahi, and A.M. Knight. A review of power converter topologies for wind generators. *IEEE International Conference on Electric Machines and Drives, 2005*, 458-465, (2005).
- [14] Z. Chen and E. Spooner. Grid power quality with variable speed wind turbines. *IEEE Transactions on Energy Conversion*, **16**(2), 148-154, (2001).
- [15] A.M. Knight and G.E. Peters. Simple Wind Energy Controller for an Expanded Operating Range. *IEEE Transactions on Energy Conversion*, **20**(2), 459-466, (2005).

- [16] Z. Chen and E. Spooner. Grid interface options for variable-speed, permanent-magnet generators. *IEE Proceedings - Electric Power Applications*, **145**(4), (1998).
- [17] K. Deb, A. Pratap, S. Agarwal, and T. Meyarivan. A Fast and Elitist Multiobjective Genetic Algorithm: NSGA-II. *IEEE Transaction on Evolutionary Computation*, **6**(2), 182–197, april 2002.
- [18] R.H. Leary, Global optimization on funneling landscapes, *J. of Global Optimization*, **18**(4), 367–383, Dec. (2000).